Reconstruction of an Acid Water Spill in a Mountain Reservoir

Rodolfo Jofre-Meléndez [1],*, Ester Torres [2], Yann René Ramos-Arroyo [1], Laura Galván [3], Carlos Ruiz-Cánovas [3] and Carlos Ayora [2]

[1]   Engineering Division, University of Guanajuato, Av. Juarez 77 Centro P.C., 36000 Guanajuato, Gto., Mexico; yr.ramos@ugto.mx
[2]   Institute of Environment Assessment and Water Research (IDAEA), CSIC, C/Jordi Girona 18-26, 08034 Barcelona, Spain; ester.torres@idaea.csic.es (E.T.); cayora1@gmail.com (C.A.)
[3]   Department of Geodynamics and Paleontology, Faculty of Experimental Sciences, University of Huelva, 21071 Huelva, Spain; laura.galvan@dgyp.uhu.es (L.G.); carlos.ruiz@dgeo.uhu.es (C.R.-C.)
*   Correspondence: jofre2525@gmail.com; Tel.: +52-473-737-5882

Abstract: The Olivargas Reservoir is located in a remote and scarcely monitored area in the Odiel River Basin (Southwest Spain) and is used for domestic, agricultural and mining water supplies. In contrast with highly monitored reservoirs, this paper explores the application of the CE-QUAL-W2 model, that was designed by Cole and Wells in 2005, to a poorly monitored reservoir and the utility of the results obtained. The model satisfactorily reproduced the water head measured continuously over three years, temperature (T), total dissolved solids (TDS), dissolved oxygen (DO) and pH measured bimonthly in a depth profile near the dam. A significant increase in TDS and decrease in DO and pH profiles were observed for four months, especially in the hypolimnion. The model reproduced changes in the parameters by assuming the occurrence of an acid water spill into the reservoir. A comparison of calculated results and measured TDS and DO prompted the conclusion that the spill consisted of approximately 3000 t of TDS (mainly sulfates) and 26 t of Fe(II) flowing into the reservoir for approximately 15 days at rates of approximately two and 0.02 kg/s, respectively.

Keywords: CE-QUAL-W2; acid water spill; Olivargas Reservoir; water reservoir management

1. Introduction

In semi-arid regions, the water supply for drinking and activities that support the economy (livestock, agriculture, industry and mining) is often limited. Moreover, if the geology does not favor the exploitation of groundwater, reservoirs are the only available water resource. Therefore, the appropriate management of both the quantity and quality of stored water is necessary for ensuring a safe supply. The efficient management of lakes and water reservoirs requires tools that can describe their complex functions and predict their behavior under changing conditions (pollutant discharge, remediation actions, climate change, etc.). Different approaches to hydrodynamic modeling have been proposed in the literature for addressing quantity and quality problems in water reservoirs [1]. The CE-QUAL-W2 model, hereinafter referred to as W2 [2,3], was originally designed to predict aspects of reservoir, lake, river and estuary management. There have been many studies on its use, most commonly to describe thermal stratification in the water column in large reservoirs [4–10]. This model has also been used to describe direct and diffusive sources of pollution [11–15], eutrophication and its evolution [16–19] and to make predictions of turbidity under different climate and management scenarios [20–25]. Efforts have involved coupling W2 with output files from hydrological models, such as the Soil and Water Assessment Tool (SWAT) [7,14,26]. It is important to note that all of these works and model

applications are based on a broad understanding of reservoir geometry and time-series data on flow, temperature profiles and chemical and biological quality.

Many small reservoirs (<50 hm^3), however, exist in remote and mountainous areas. They supply water to small communities, and there is rarely accurate monitoring or complete datasets on their physical, chemical and biological parameters. For such communities, water resource management is just as necessary, but the application of the conventional W2 can be challenging and has yet not been explored.

The present work describes the calibration of the W2 model for a small reservoir with scarce monitoring in the upper basin of the Odiel River (in Southwest Spain). This region is known for its mining activity, and water from the reservoir is used for domestic consumption, agriculture and mining. As the only form of surveillance, a depth profile of temperature (T), electric conductivity (EC), dissolved oxygen (DO), pH and oxidation-reduction potential (ORP) was taken every two months close to the dam of the reservoir from June 2009 to December 2012. All these data were obtainable by the user without permanent stations or monitoring programs. Besides, an anomalous EC, DO and pH values were detected in one surveillance campaign and were attributed to a possible mining spill.

For the reconstruction and evaluation of a possible pollution event, a W2 model was built and calibrated with the data from the bimonthly profiles. In contrast with the highly detailed models on highly monitored reservoirs, this paper explores the application of W2 to a poorly monitored reservoir and the utility of the results obtained.

2. Study Site Description

The Olivargas Reservoir is located in the Odiel River Basin in southwestern Spain at 37°42′44″ N, 6°48′29″ W and 127 m above sea level (m a.s.l.) with a longitudinal shape (Figure 1). Its main uses include supplying the Aguas Teñidas mine and providing domestic water for the villages of La Zarza and Perrunal (3600 habitants). Recently, the reservoir has been used for irrigation and to supply water to the population of Calañas (4200 habitants), located downstream. Table 1 summarizes some of the main characteristics of the reservoir.
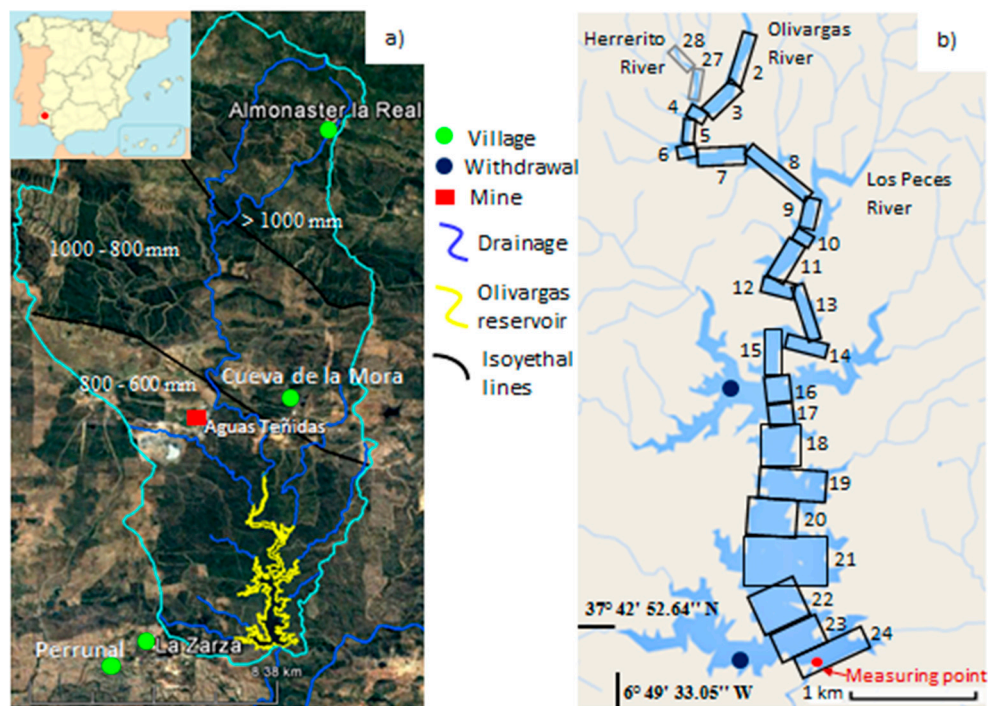

Figure 1. (**a**) Location of Olivargas River Basin; (**b**) Segments of reservoir discretization.

Table 1. Main characteristics of the Olivargas Reservoir.

Variable	Value
Dam crest height *, m a.s.l.	163
Volume *, Mm^3	28.5
Total area *, km^2	2.44
Maximum depth *, m	33
Length *, km	7.57
Greatest width *, km	1.6
Spillway height, m a.s.l.	158.7
Number of withdrawal structures	2
Average percent for mining extraction, %	45
Average percent of extraction for domestic supply, %	55
Year of filling	1983

Note: * yearly averaged.

The Huelva Province (in Southwest Spain) has a dry Mediterranean climate that is characterized by great inter- and intra-annual variation in rainfall distribution. In fact, 80% of the annual rainfall occurs between October and March (Figure 2). The area is also affected by recurrent droughts [27].
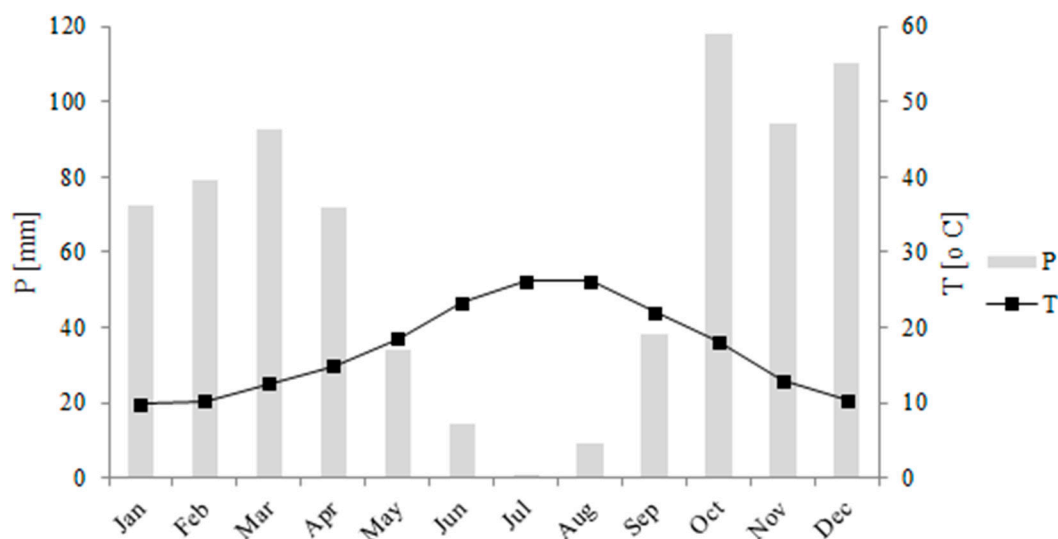

Figure 2. Average precipitation (mm) and temperature (°C) from 2000 to 2015 at El Campillo Station (406 m a.s.l.), located 19.25 km from the reservoir.

The Olivargas Reservoir is fitted by three main effluents: the Olivargas, Los Peces and Herrerito streams (Figure 1b). The main channel is the Olivargas River, which, in the rainy season (October to April), contributes more than 90% of the incoming water [28]. The geology of the catchment area is made up of metamorphic siliciclastic rocks without carbonates [29]. Three abandoned mines and one active site of massive pyrite body extraction (the Aguas Teñidas mine) are located in the area (Figure 1a).

3. Materials and Methods

3.1. On-Site Measurements

For the continuous control of water head, T and EC, three CTD-DIVERs were installed in the three main incoming streams of the reservoir (Olivargas, Herrerito, and Los Peces). Near the dam of the reservoir, a DIVER was installed for the determination of water head, and a BaroDiver was used to compensate head measurements with atmospheric pressure. Measurement periods in the three streams were from 15 September 2009 to 21 October 2011, and 14 April to 18 September 2012.

Measurement periods in the reservoir were from 4 June 2009 to 3 February 2010; 18 June to 10 October 2010; and from 24 November 2010 to 4 July 2011. The installed sensors were manufactured by Schlumberger (accuracy: T ±0.1 °C, EC ±01%, pressure ±0.1%).

Similarly, between July 2009 and December 2012, vertical profiles were taken near the dam approximately once every two months (Figure 1b). There, temperature, EC, DO, pH and ORP were measured for every meter of depth using a SEBA HYDROMETRIE KLL-Q multi-parametric probe (accuracy: T ±0.1 °C, EC ±0.5%, DO ±0.5%, pH ±0.1, ORP ±2 mV). Certified commercial standards were used to calibrate the equipment. During the instrumentation, four sampling campaigns along the reservoir were conducted, during which major anions and cations, alkalinity and dissolved organic carbon (DOC) were determined in addition to the above parameters.

3.2. Model Description and Application

3.2.1. General Model Description

The W2 v. 4.0 model is a two-dimensional (longitudinal-vertical) hydrodynamic and water quality model, which assumes homogeneity along the lateral direction [3]. W2 uses a finite difference approximation to solve implicit equations of fluid movement, including free surface, hydrostatic pressure, horizontal and vertical moment, continuity, transport of constituents and water state equations. Moreover, W2 provides a numerical scheme, ULTIMATE, for the advection term of the mass transport equation to eliminate numerical dispersion and oscillation [2]. This is particularly important in successfully reproducing DO stratification in the water column by accurately quantifying vertical advective mass transport.

The water quality algorithm incorporates 21 state variables, including T, salinity, DO, algae, total phosphorus, ammonia and a conservative tracer, but only the first three were used here. It also includes 60 derived variables, including pH, total organic carbon, DOC, total organic nitrogen and dissolved organic phosphorus, that can each be calculated internally from state variables and compared with measured data.

3.2.2. Geometry and Bathymetry Derivation

The Olivargas Reservoir is oriented north-south and is composed of three branches corresponding to three main incoming streams; although, only the Olivargas River makes an important contribution to the reservoir. Thus, the strategy for adjusting the geometry of the reservoir to the W2 input file entailed adapting one branch along the main axis (Figure 1b).

For obtaining the bathymetry, old topographic maps were used as reference. Besides, water depth was measured at 13 points along the axis of the reservoir. These measured depth values allowed the derivation of a relationship between the distance from the entry point and the reservoir depth (Figure 3a), as follows:

$$y = 3 \times 10^{-7}x^2 - 0.0064x - 1.183 \ (R^2 = 0.9552) \tag{1}$$

Finally, the bathymetry in the W2 model was adjusted to 24 longitudinal segments ranging from 90 to 790 m in length and 50 to 660 m in width. The vertical discretization of the layers of each segment was 1 m, reaching a maximum of 32 layers in the deepest areas near the dam (Figure 3b). A semi-ellipsoidal channel shape was considered for adjusting the variation in the width of layers (Figure 3c). A maximum time-step of 600 s was set in the model simulations, with a model computed average time-step of 200 s.
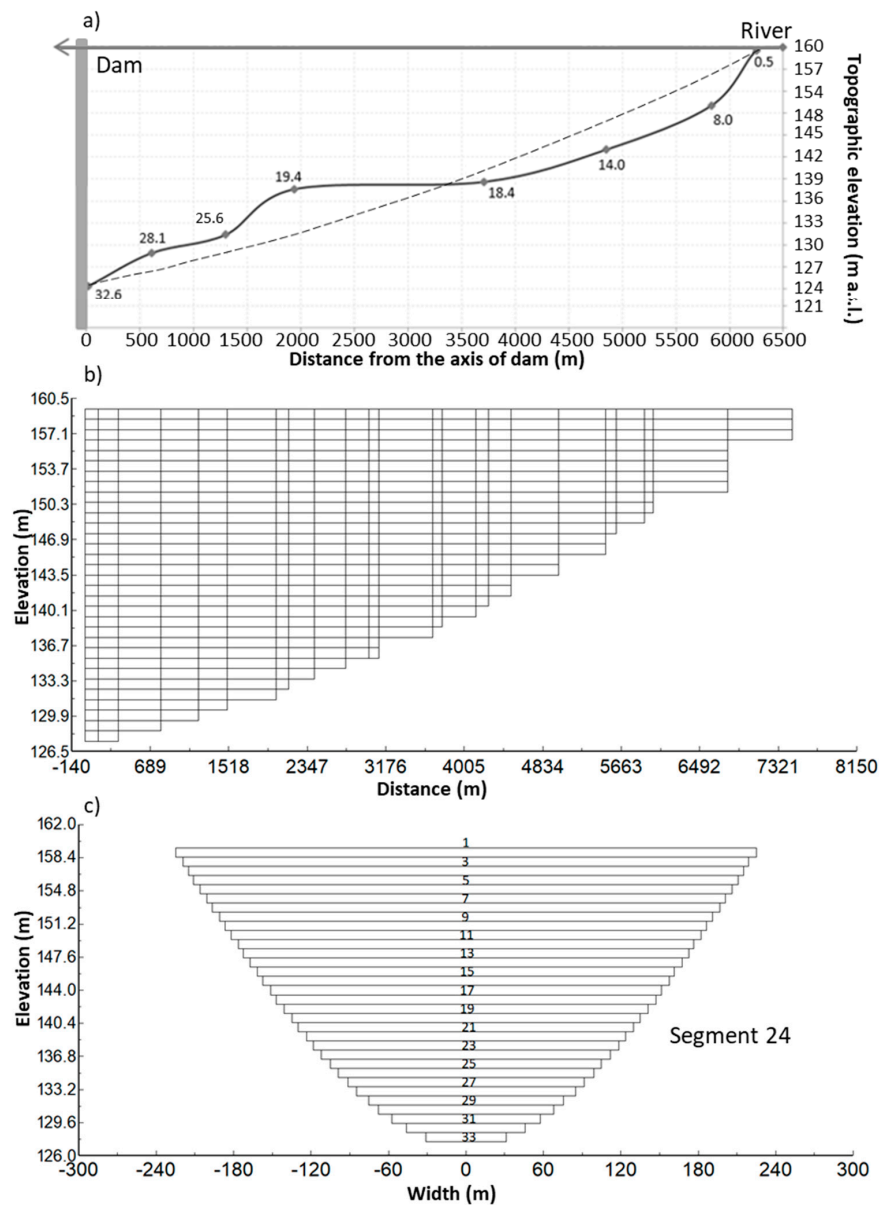
Figure 3. (**a**) Longitudinal section of the Olivargas Reservoir used to derive the bathymetry (solid line) and adjusted bathymetry (dashed line); (**b**) Longitudinal section of branch 1; (**c**) Vertical section of segment 24 of Figure 1b, where the horizontal layers can be observed.

3.2.3. Data Sources

The simulation was continuously run for 43 months from 1 June 2009 (Julian day, JD = 152) to 31 December 2012 (JD = 1461), during which period the instrumentation and sampling were implemented at the study site. 1 January 2009, was taken as JD = 1.

The following boundary conditions were set:

- Meteorological data: Air temperature, relative humidity, wind speed and direction, precipitation and solar radiation data were obtained from the Meteorological Spanish Survey [30] from El Campillo Station, located 19.25 km east of the Olivargas Reservoir. Dew point temperature was calculated from relative humidity and air temperature [31]. The precipitation temperature was obtained from the dew point. The percentage of cloud cover was calculated according to the methods of [32–34] from the solar radiation data, with Glover and McCulloch's method providing the best result.

- Flow into the reservoir: The only inflow considered was from the Olivargas River, which, in the rainy season, contributes more than 90% of the incoming flow. The river flow database was generated with the SWAT code. A more detailed description of the SWAT model application to the region can be found in [28,35,36].
- Inflow water quality:

  ○ The water temperature of the inflow was obtained from continuous measurements by the CTD-DIVER installed in the Olivargas River.
  ○ The total dissolved solids (TDS) of the inflow was calculated from the EC measured continuously by a CTD-DIVER installed in the Olivargas River and the molecular weight of $CaSO_4$ (the dominant salt in the reservoir).
  ○ The DO of the inflow was calculated from the air-water equilibrium, water temperature and ionic strength.
  ○ The labile dissolved organic matter (LDOM) and the alkalinity of the inflow were obtained from the average of four sampling campaigns and considered constant throughout the modeling period. Total inorganic carbon (TIC) was obtained from the measured values of pH and alkalinity.

- Extractions: There are two water withdrawal points instrumented inside the reservoir: one for the mining company, MATSA, operating the Aguas Teñidas mine located near segment 16, and another owned by the drinking water company, GIAHSA, located near segment 23 (blue dots, Figure 1b).

In addition, the following initial conditions were set:

- Temperature, TDS, and DO profiles were taken at the measuring point near the dam (Figure 1b) on the 6 July 2009.
- The LDOM profile was obtained at the measuring point on 30 January 2010.
- The alkalinity profile was obtained on 4 September 2009, at the measuring point. The TIC profile was obtained from the alkalinity and pH values.

There were periods in which no data from the inflow water were available because the instrument deteriorated when the river dried. These periods were from 1 June to 14 September 2009; 22 October 2011 to 13 April 2012; and 19 September to 31 December 2012. The following methods were used to estimate the absent data:

- Water temperature was estimated from mean air temperature measured in the reservoir or at El Campillo Station with the formula from [37].
- Electric conductivity was estimated from the correlations between measured EC and flow data from the Olivargas River in the rainy and dry seasons (Figure 4).
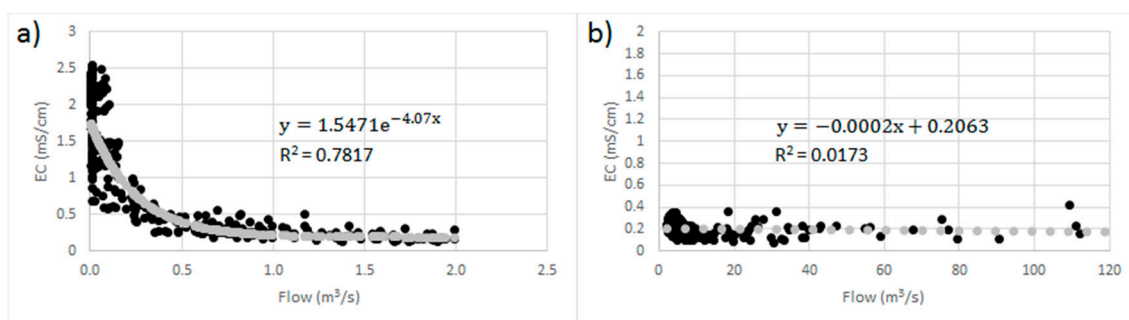

Figure 4. Correlation between the EC and flow values from the Olivargas River: (**a**) for dry season (flow <2 m^3/s) and (**b**) for rainy season (flow >2 m^3/s). Black dots are recorded values, and gray dots are the adjustment trend.

4. Results and Discussion

4.1. General Calibration of Model

Data profiles of temperature, EC, pH and ORP measured bimonthly near the dam from June 2009 to June 2012 were used for the model calibration. The W2 hydrodynamics calibration also included the parameters presented in Table 2. All the calibrated parameters fell within or very close to the range of the default values given by [3]. In estimating the fitness between the predicted and observed values, the mean absolute error (MAE) was calculated for each realization, and also the percentage relative error (PRE) and the root mean square error (RMSE) were obtained [38].

Table 2. Calibration parameters used (bold indicates parameters chosen based on sensitivity analysis).

Coefficient	Olivargas Reservoir	Cole and Wells (2015)
Horizontal eddy viscosity, m^2/s	1.0	1.0
Horizontal eddy diffusivity, m^2/s	1.0	1.0
Interfacial friction factor, *adim*	0.015	0.015
Manning coefficient, $s/m^{1/3}$	0.027	-
Wind roughness height, m	0.001	0.001
Wind sheltering, *adim*	**1.2**	**0.1–0.9**
Fraction of heat lost to sediments added back to water column, *adim*	1.0	1.0
Fraction of solar radiation absorbed at the water surface, *adim*	0.45	0.45
Coefficient of bottom heat exchange, $W/m^2/s$	0.3	0.3
Light extinction coefficient for pure water, m^{-1}	0.45	0.25 or 0.45
Extinction coefficient for inorganic solid, m^{-1}	0.1	0.1
Extinction coefficient for organic solid, m^{-1}	0.1	0.1
LDOM decay rate, day^{-1}	0.1	0.1
Sediment oxygen demand, $g/m^2/day$	**0.2**	**0.1–0.5**

4.2. Hydrodynamic Modeling

4.2.1. Water Head

For calibration of the water surface elevation, the evolution of water balance in the reservoir was used (Figure 5) via the Mass Balance Utility version 3.7 of W2, which added or removed water from the system to fit the calculated to the observed levels. In addition, the calibration parameters, the α1 and β1 coefficients, representing water head versus flow for freely flowing conditions, were adapted depending on the spillway shape [3]. It was noted that between 2011 and 2012, a moderate drought occurred, and the reservoir level remained mostly below the spill level (Figure 5).

The water residence time is approximately one year. The winter storms of the Mediterranean climate cause the complete filling of the water reservoir in approximately seven days, the river water is colder than the reservoir water, and the incoming water is placed at the bottom. However, in the spring, the river water is hotter and is placed at the surface of the reservoir, and the surface water is newer than the bottom water, which is gradually ordered in depth.

Figure 6 shows that the calculated water heads matched the measured values well in both the dry and rainy periods. The model perfectly captured the water level increase generated by various floods in the rainy season in winter, in which great floods occur (flow >10 m^3/s). In winter, the incoming water was colder than the reservoir water. It, therefore, occupied the bottom of the reservoir, pushing older water up and causing water to mix approximately 17 days after a great flooding event.
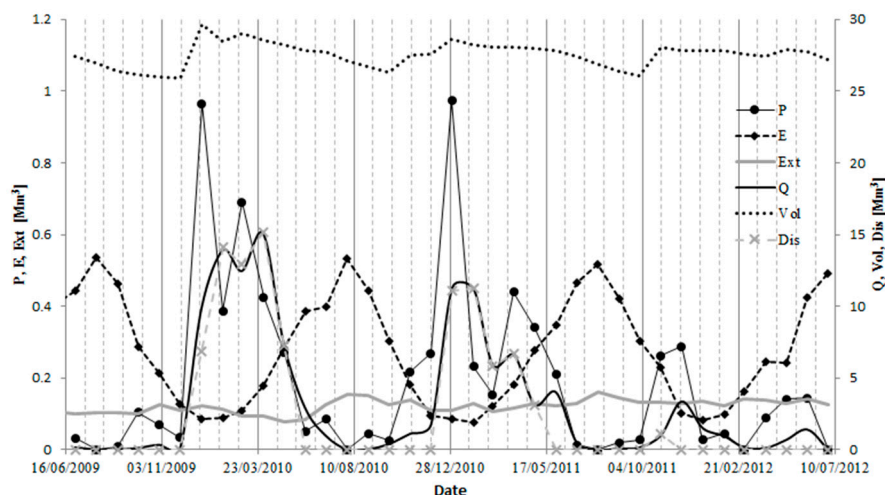
Figure 5. Evolution of the water balance in the Olivargas Reservoir. P is precipitation (measured), E is evaporation (obtained with W2), Ext is extractions (measured), Q is the water mass flowing into the reservoir (obtained with SWAT), Vol is the volume of the reservoir (obtained with W2), and Dis are discharges from the reservoir (obtained with W2). All the parameters are represented in Mm^3.
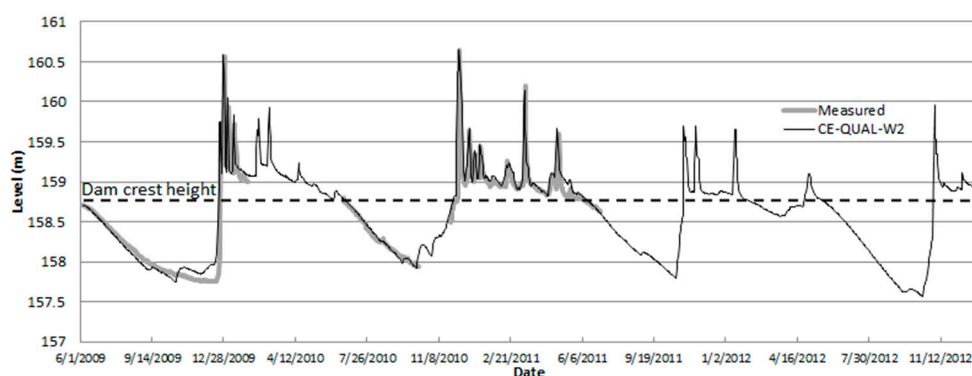

Figure 6. Water surface elevations in the Olivargas Reservoir. The black line represents the calculated values, and the gray line corresponds to the measured data. The dashed line represents the spillway level.

4.2.2. Temperature

Cloudiness and wind sheltering were used as calibration parameters. The sediment temperature was set to 10 °C, the default value given by [3].

As shown by the MAE value of each graph, the model satisfactorily reproduced the data measured in the profile near the dam (Figure 7) and the thermal stratification (dry season) and mixing (rainy season). Besides, in most of cases the PRE and the RMSE are lower than 10% and 2.5 °C respectively. However, a difference of 2.5 m in the thermocline depth was observed in the stratification periods. This may have been caused by an excess of wind in the water surface, as the meteorological data used in the model were from the closest station, which is 19.25 km from the reservoir, and by uncertainty in the bathymetric data, which were roughly approximated.
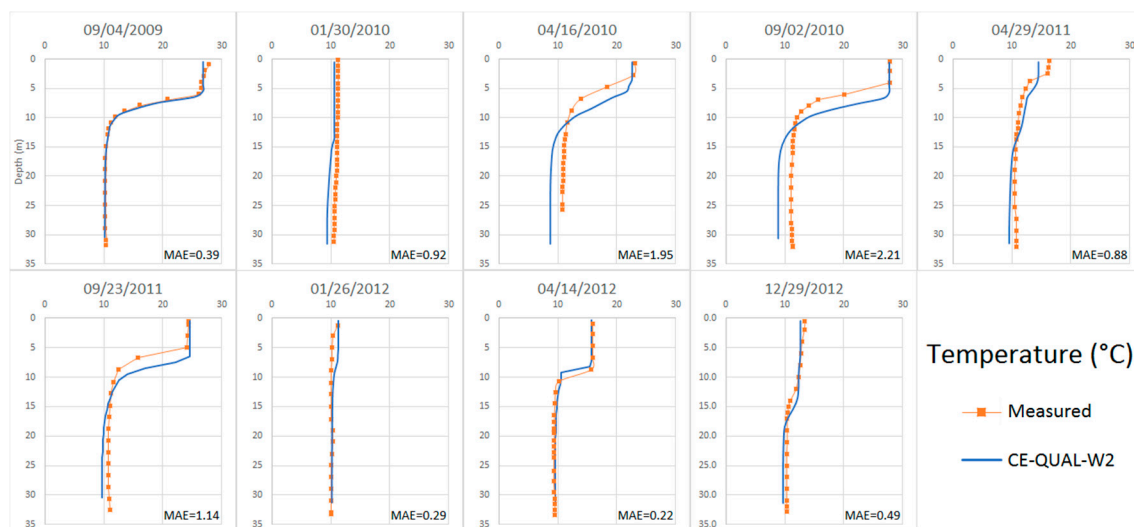
Figure 7. Temperature distribution profiles for different dates in dry and rainy seasons near the dam of the Olivargas Reservoir.

4.2.3. Total dissolved solids (TDS)

Figure 8 shows measured and calculated TDS profiles on the dam for each dry and rainy season within the simulated period. In calibrating the TDS, a "first flood" factor was considered. This factor impacts the salinity of the first flooding event (the first rain), taking into account the salt dissolution that precipitated into the river during the dry season. After this first flood, which dissolves all of the salts on the riverbed, salinity decreases due to increasing flow [39].

Until January 2012, the model satisfactorily predicted the TDS distribution with low MAE (Figure 8). PRE and RMSE are also low with maximum values of 15% and 28 g/m^3 respectively. However, after 26 January 2012, the measurements exhibited an obvious increase in TDS that the model failed to predict and which was more pronounced in the hypolimnion. This increase suggests an inflow of water with a TDS higher than usual, as discussed below. These anomalous TDS values persisted until the end of May and then subsided. The measured and predicted values had returned to normal by December 2012.
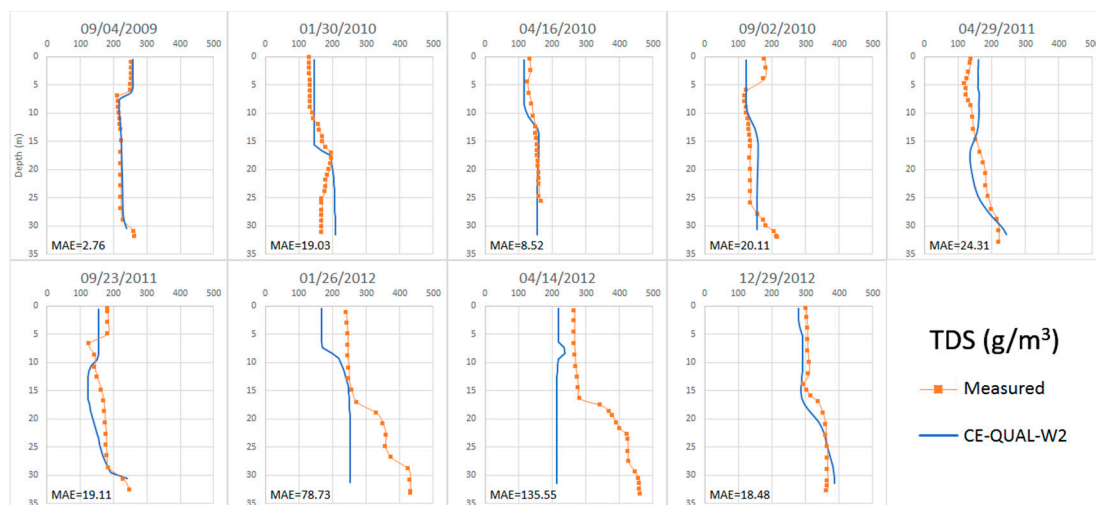

Figure 8. Total dissolved solids (TDS) distribution profiles for different dates in dry and rainy seasons near the dam of the Olivargas Reservoir.

4.2.4. Dissolved Oxygen

The DO concentration in reservoirs is primarily linked to sediment oxygen demand (SOD), the decomposition of organic matter and oxygen production via photosynthesis by algae. Under hypoxic conditions in the pore water, Fe^{2+}, Mn^{2+}, S^{2-} and As^{3+} can be released from sediments. This process consumes DO from the hypolimnion, and water quality decreases [40].

SOD (which remained constant in all segments) and the time series of LDOM were used as calibration parameters for DO. The calculated values did not fit the measurements as accurately as with temperature and TDS (Figure 9). Thus, in the dry season, the measured DO concentration exhibited an increase between the epilimnion and the metalimnion, which was not predicted by the model. This was due to algae photosynthesis, whereas the algae module was not active in the model because no measurements of algae concentration were available. However, until January 2012, a low MAE, PRE and RMSE were still achieved with maximum values of 3 g/m^3, 20% and 2.7 g/m^3 respectively.

Interestingly, parallel to the TDS increase, a clear drop in measured DO values in the hypolimnion was measured on 26 January 2012, which the model failed to predict. There was a clear increase in oxygen consumption at 20 m of depth, leaving the hypolimnion anoxic; however, the model was unable to reproduce this. After the end of May, the measured and calculated values tended to reflect the values from prior to January. Again, the results suggest an intrusion of a different kind of water, which consumed oxygen in addition to adding TDS to the hypolimnion.
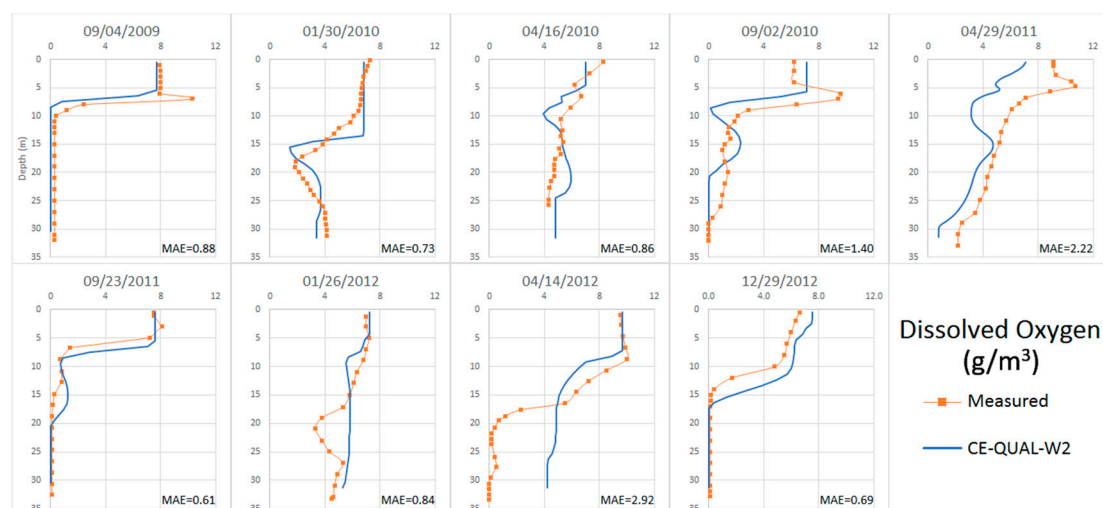

Figure 9. Dissolved oxygen (DO) distribution profiles for different dates in the dry and rainy seasons from a profile near the dam of the Olivargas Reservoir.

4.2.5. pH

Figure 10 shows that the model matched the measured pH values. However, the W2 was unable to predict an increase in pH at the sediment interface; this occurs because Fe(III) is reduced to Fe(II) via the consumption of protons from the water, which is not considered by the model in the calculation of pH (Equation (2)).

Concomitant with the TDS increase and DO drop, a progressive decrease in pH was measured from January to May 2012 that the model was unable to predict. After May, the pH tended toward the values prior to January. Regarding TDS and DO, this pH trend in 2012 suggests the occurrence of an abnormal process that released protons to the hypolimnion. Except this anomalous period, MAE, PRE and RMSE present low values (around of 0.58, 8% and 0.6 respectively).
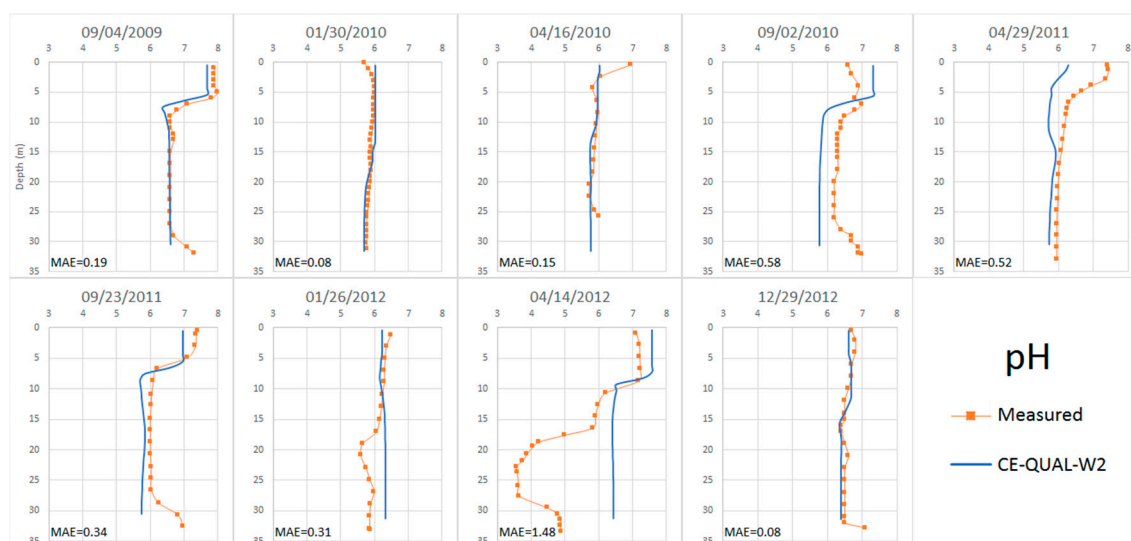
Figure 10. pH distribution profiles for different dates in dry and rainy seasons from a profile near the dam of the Olivargas Reservoir.

4.3. Calibration of the Anomalous Period

As described in the previous sections, the model was unable to reproduce the profiles of TDS, DO and pH between January and May 2012. A possible explanation is that a spill of contaminated acid water with high TDS and Fe(II) content reached the reservoir in the days prior to 26 January 2012. Fe(II), a common solute in acid mine drainage, would have oxidized to Fe(III), consuming the DO, and the Fe(III) would have hydrolyzed the water, releasing protons. This anomalous period was modeled via the addition of a new input as a new branch to the model geometry (segments 27 and 28, Figure 1b). This water inflow had a temperature equal to that of the Olivargas River with higher TDS; thus, the model was adjusted by the addition of Fe(II) to consume the dissolved oxygen. The spill water would have been denser than the water of the reservoir and would have circulated below the epilimnion.

For estimation of the TDS in the spill, the difference between the total solute charge measured in the reservoir and that predicted by the model (Figure 8, 26 January 2012) was calculated. The total amount of solutes in the reservoir was quantified with assumed longitudinal TDS homogeneity and the volume per meter of depth depending on the bathymetry. Total solute masses of 8412 and 5550 t were estimated for measured and predicted TDS values in the reservoir, respectively. Therefore, a total mass of 2862 t of TDS was assigned to the spill.

For determination of the time period in which the event could have occurred, the total TDS of the spill was distributed within periods of one day to three months. The end of the spill period was set to 26 January 2012, the date of first detection. A maximum flow rate of 0.92 m^3/s was allowed during the spill period, which is twice the average flow of the Olivargas River in January, previous to the detection of the pollution event. Higher flow values could have caused alarm in the village of Cueva de la Mora near the Olivargas River. For simulations the total spilled mass and the flow rate were fixed, and ranges of TDS concentrations between 36,000 g/m^3 for one day of simulation and 400 g/m^3 for 90 days of simulation were used.

The simulated and measured TDS profiles were compared under different possible durations of the spill until the lowest possible MAE was achieved. After several trials, a spill duration of 15 days was selected as the best scenario. For adjusting the DO, the averaged Fe(II) value measured in the acidic streams of the catchment area [41] was used as the initial value of the calculations and was adjusted until the DO profiles attained the lowest MAE.

Three durations of 1, 15 and 90 days for the spill were compared (Figure 11). Figure 11a (green dashed line) shows the simulation if the entire mass of the spill flowed into the reservoir in only 1 day.

The TDS was consistently underestimated in the epilimnion and part of the metalimnion (above 20 m deep); however, it was always overestimated in the hypolimnion (below 20 m deep). This is because the incoming water was so dense that it immediately sank and mixing in the epilimnion was not possible. Figure 11a (blue dots) shows the calculation if the mass of spill was distributed and received continuously over 90 days. In this case, the predicted TDS concentration was always lower than the measured one.

Consumption of DO due to the spill was clearly observed in all calculated scenarios (Figure 11b). Further, different durations of the spill did not significantly change the DO (there were very similar MAE values). When the spill lasted one day (green dashed line), the DO consumed was slightly higher than the observed value, while when the event lasted three months (blue dots), it was less than that observed, especially at the bottom. It is important to note that the temperature did not exhibit significant changes with the spill event.

Once the spill duration was calibrated, different start dates for the spill were tested until the best fit with the measured profiles was achieved. Finally, the best adjustment (minimum MAE) was obtained for the 15-day period from 10 to 24 January 2012 (Figure 11, red solid line), which produced a TDS mass flow of 2.21 kg/s and a total Fe(II) mass of 26.2 t (mass flow of 0.02 kg/s). For an averaged flow rate of 0.46 m³/s in the Olivargas River during the spill period, the TDS and Fe(II) concentrations were estimated as 5 g/L and 50 mg/L, respectively. Such a TDS value is common in the acidic mine drainage of the region [41,42], while the Fe(II) concentration falls within the lower end of the range measured in the acidic mine drainage. However, the estimated concentration represents the minimum Fe(II) necessary to account for the DO consumed in the hypolimnion.
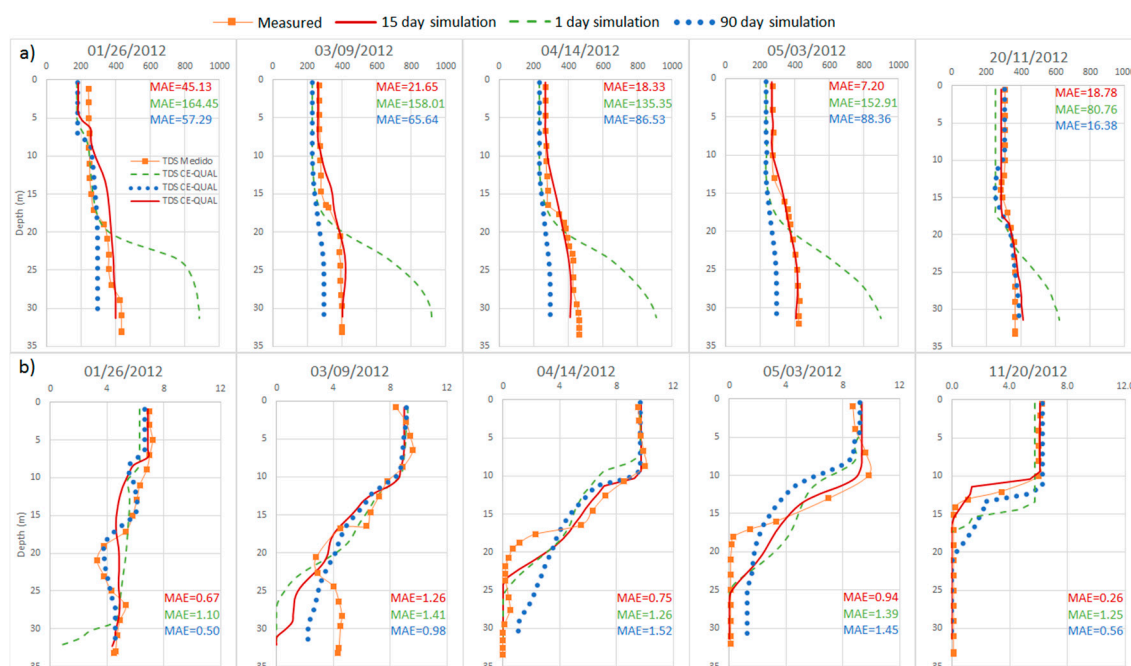

Figure 11. Vertical profiles near the dam of the Olivargas Reservoir for different durations of a spill event: (**a**) TDS (g/m³); (**b**) DO (g/m³).

Version 4.0 of W2 calculates the pH based on a carbonate system. In a possible event produced by acidic mine discharge, a large amount of sulfates and metals, such as Fe, Al, Mn, etc. could have been discharged into the reservoir [27]. The oxidation of Fe and precipitation of schwertmannite could have released a large amount of protons into the water, which are not considered by W2 version 4.0, as shown in the following equation:

$$8Fe^{2+} + SO_4^{2-} + 2O_2 + (10 + n)H_2O \rightarrow Fe_8O_8(OH)_6SO_4 \cdot nH_2O + 14H^+ \tag{2}$$

As with Fe, additional reactions, such as aluminum hydrolysis and precipitation of basaluminite ($Al_4(SO_4)(OH)_{10} \cdot 4H_2O$), are not considered by the model [13]. Thus, during the spill event, measured pH, especially in the hypolimnion, was between one and three units below the value predicted by the model.

5. Conclusions

The W2 model satisfactorily reproduced the water level, temperature, TDS, DO and pH continuously from June 2009 to January 2012, including changes in stratification and mixing periods in the reservoir. This reproduction was achieved even though the location was a remote and mountainous area with poor monitoring and control. The instrumentation used was likely the minimum required for use of the W2 as a model for sustainable management.

From January to May 2012, a significant increase in TDS and decrease in DO and pH were observed, especially in the hypolimnion. The W2 model also reproduced the changes in these parameters by assuming the occurrence of an acid water spill into the reservoir. A comparison of calculation results and the TDS and DO data measured in a profile near the dam prompted the conclusion that the spill consisted of approximately 3000 t of TDS (mainly sulfates) for approximately 15 days (during January 2012) with a rate of approximately 2 kg/s. The spill further likely contained a minimum of 27 t of dissolved Fe(II) with a rate of 0.02 kg/s. Approximately seven months after the spill, the reservoir had already recovered its TDS, DO and pH to the levels observed prior to the event.

The W2 is limited in calculating the pH, since it considers the oxidation of Fe(II) and the precipitation of minerals, such as iron hydroxides; however, it does not consider the protons released in the reactions in pH calculations.

Author Contributions: Rodolfo Jofre-Meléndez did the application and calibration of CE-QUAL-W2 model, the reconstruction of the acid water spill, the scientific research, and the paper redaction. Ester Torres supported in the calibration of CE-QUAL-W2 model, the adaptation of the diagenesis process in the CEQUAL-W2 model, and the scientific review. Yann René Ramos-Arroyo: made the bathymetry derivation, supported in water balance and scientific review. Laura Galván did the application and calibration of the SWAT model, measured field variables and did flow correlations. Carlos Ruiz-Cánovas: did field instrumentation, on-site measurements, and database management. Carlos Ayora: did the hydrogeochemistry processes description and the main scientific review.

Conflicts of Interest: The authors declare no conflict of interest.

References

1. Mooij, W.M.; Trolle, D.; Jeppesen, E.; Arhonditsis, G.; Belolipetsky, P.V.; Chitamwebwa, D.B.R.; Degermendzhy, A.G.; De Angelis, D.L.; De Senerpont Domis, L.N.; Downing, A.S.; et al. Challenges and opportunities for integrating lake ecosystem modeling approaches. *Aquat. Ecol.* **2010**, *44*, 633–667. [CrossRef]

2. Cole, T.M.; Wells, S.A. *Hydrodynamic Modeling with Application to CE-QUAL-W2. En Workshop Notes*; Portland State University: Portland, OR, USA, 2000.

3. Cole, T.M.; Wells, S.A. *CE-QUAL-W2: A Two-Dimensional, Laterally Averaged, Hydrodynamic and Water Quality Model*; Version 4.0; Portland State Univeristy: Portland, OR, USA, 2015. Available online: http://archives.pdx.edu/ds/psu/12049 (accessed on 14 February 2015).

4. Zouabi-Aloui, B.; Adelana, S.M.; Gueddari, M. Effects of selective withdrawal on hydrodynamics and water quality of a thermally stratified reservoir in the southern side of the Mediterranean Sea: A simulation approach. *Environ. Monit. Assess.* **2015**, *187*, 1–19. [CrossRef] [PubMed]

5. Fataei, E.; Moghadam, D.A.; Nasehi, F. Prediction of thermal stratification of Seymareh Dam using CE-QUAL-W2. *Model. Adv. Bot. Res.* **2014**, *5*, 150–159. [CrossRef]

6. Wells, S.A.; Wells, V.I.; Berger, C. *Impact of Phosphorus Loading from the Watershed on Water Quality Dynamics in Lake Tenkiller, Oklahoma, USA*; World Environmental and Water Resources Congress: Sacramento, CA, USA, 2012; pp. 888–899. [CrossRef]

7. White, J.D.; Prochnow, S.J.; Filstrup, C.T.; Scott, J.T.; Byars, B.W.; Zygo-Flynn, L. A combined watershed-water quality modeling analysis of the Lake Wako reservoir: I. Calibration and confirmation of predicted water quality. *Lake Reserv. Manag.* **2010**, *26*, 147–158. [CrossRef]

8. Wu, T.; Luo, L.; Qin, B.; Cui, G.; Yu, Z.; Yao, Z. A vertically integrated eutrophication model and its application to a river-style reservoir—Fuchunjiang, China. *J. Environ. Sci.* **2009**, *21*, 319–327. [CrossRef]

9. Khangaonkar, T.; Yang, Z. Dynamic response of stream temperatures to boundary and inflow perturbation due to reservoir operations. *River Res. Appl.* **2008**, *24*, 420–433. [CrossRef]

10. Ma, S.; Kassinos, S.C.; Kassinos, D.F.; Akylas, E. Effects of selective water withdrawal schemes on thermal stratification in Kouris Dam in Cyprus. *Lake Reserv. Manag.* **2008**, *13*, 51–61. [CrossRef]

11. Afshar, A.; Masoumi, F. Waste load reallocation in river–reservoir systems: Simulation–optimization approach. *Environ. Earth Sci.* **2016**, *75*, 1–14. [CrossRef]

12. Jeznach, L.C.; Jones, C.; Matthews, T.; Tobiason, J.E.; Ahlfeld, D.P. A framework for modeling contaminant impacts on reservoir water quality. *J. Hydrol.* **2016**, *537*, 322–333. [CrossRef]

13. Torres, E.; Galván, L.; Ruiz Cánovas, C.; Soria-Píriz, S.; Arbat-Bofill, M.; Nardi, A.; Papaspyrou, S.; Ayora, C. Oxycline formation induced by Fe(II) oxidation in a water reservoir affected by Acid Mine Drainage modeled using a 2D hydrodynamic and water quality model—CE-QUAL-W2. *Sci. Total Environ.* **2016**, *562*, 1–12. [CrossRef] [PubMed]

14. Narasimhan, B.; Srinivasan, R.; Bednarz, S.T.; Ernst, M.R.; Allen, P.M. A comprehensive modeling approach for reservoir water quality assessment and management due to point and nonpoint source pollution. *Trans. ASABE* **2010**, *53*, 1605–1617. [CrossRef]

15. Yu, S.J.; Lee, J.Y.; Ryong, H.S. Effect of a seasonal diffuse pollution migration on natural organic matter behavior in a stratified dam reservoir. *J. Environ. Sci.* **2010**, *22*, 908–914. [CrossRef]

16. Noori, R.; Yeh, H.D.; Ashrafi, K.; Rezazadeh, N.; Bateni, S.M.; Karbassi, A.; Kachoosangi, F.T.; Moazami, S. A reduced-order based CE-QUAL-W2 model for simulation of nitrate concentration in dam reservoirs. *J. Hydrol.* **2015**, *530*, 645–656. [CrossRef]

17. Park, Y.; Cho, K.H.; Kang, J.H.; Lee, S.W.; Kim, J.H. Developing a flow strategy to reduce nutrient load in a reclaimed multi-reservoir system using a 2D hydrodynamic and water quality model. *Sci. Total Environ.* **2014**, *466*, 871–880. [CrossRef] [PubMed]

18. Berger, C.J.; Wells, S.A. Modeling the effects of macrophytes on hydrodynamics. *J. Environ. Eng.* **2008**, *134*, 778–788. [CrossRef]

19. Kuo, J.T.; Lung, W.S.; Yang, C.P.; Liu, W.C.; Yang, M.D.; Tang, T.S. Eutrophication modeling of reservoirs in Taiwan. *Environ. Model. Softw.* **2006**, *21*, 829–844. [CrossRef]

20. Buccola, N.L.; Risley, J.C.; Rounds, S.A. Simulating future water temperatures in the North Santiam River, Oregon. *J. Hydrol.* **2016**, *535*, 318–330. [CrossRef]

21. Molina-Navarro, E.; Trolle, D.; Martínez-Pérez, S.; Sastre-Merlín, A.; Jeppesen, E. Hydrological and water quality impact assessment of a Mediterranean limno-reservoir under climate change and land use management scenarios. *J. Hydrol.* **2014**, *509*, 354–356. [CrossRef]

22. Lee, C.; Foster, G. Assessing the potential of reservoir outflow management to reduce sedimentation using continuous turbidity monitoring and reservoir modelling. *Hydrol. Process.* **2013**, *27*, 1426–1439. [CrossRef]

23. Samal, N.R.; Matonse, A.H.; Mukundan, R.; Zion, M.S.; Pierson, D.C.; Gelda, R.K.; Schneiderman, E.M. Modelling potential effects of climate change on winter turbidity loading in the Ashokan Reservoir, NY. *Hydrol. Process.* **2013**, *27*, 3061–3074. [CrossRef]

24. Choi, J.H.; Jeong, S.A.; Park, S.S. Longitudinal-vertical hydrodynamic and turbidity simulations for prediction of dam reconstruction effects in Asian monsoon area. *J. Am. Water Resour. Assoc.* **2007**, *43*, 1444–1454. [CrossRef]

25. Bowen, J.D.; Hieronymus, J.W. A CE-QUAL-W2 model of Neuse Estuary for total maximum daily load development. *J. Water Resour. Plann. Manag.* **2003**, *129*, 283–294. [CrossRef]

26. Debele, B.; Srinivasan, R.; Parlange, J.Y. Coupling upland watershead and downstream waterbody hydrodynamic and water quality models (SWAT and DE-CUAL-W2) for better water resources management in complex river basins. *Environ. Model. Assess.* **2008**, *13*, 135–153. [CrossRef]

27. Cánovas, C.R.; Olías, M.; Macias, F.; Torres, E.; San Miguel, E.G.; Galván, L.; Ayora, C.; Nieto, J.M. Water acidification trends in a reservoir of the Iberian Pyrite Belt (SW Spain). *Sci. Total Environ.* **2016**, *541*, 400–411. [CrossRef] [PubMed]

28. Galván, L.; Olías, M.; Cánovas, C.R.; Sarmiento, A.M.; Nieto, J.M. Hydrological modeling of a watershed affected by acid mine drainage (Odiel River, SW Spain). Assessment of the pollutant contributing areas. *J. Hydrol.* **2016**, *540*, 196–206. [CrossRef]

29. Tornos, F. Environment of formation and styles of volcanogenic massive sulfides: The Iberian Pyrite Belt. *Ore Geol. Rev.* **2006**, *28*, 259–307. [CrossRef]

30. Agencia Estatal de Meteorología, *AEMET*. Spain. Available online: http://www.aemet.es (accessed on 22 May 2015).

31. Hess, S.L. *Introduction to Theoretical Meteorology*, 1st ed.; Holt, Rinehart, and Winston: New York, NY, USA, 1978; p. 362. ISBN 0882758578.

32. Prescott, J. Evaporation from a water surface in relation to solar radiation. *Q. J. R. Meteorol. Soc.* **1940**, *64*, 114–118.

33. Glover, J.; McCulloch, J.S.G. The empirical relation between solar radiation and hours of sunshine. *Q. J. R. Meteorol. Soc.* **1958**, *84*, 172–175. [CrossRef]

34. Black, J.N. The distribution of solar radiation over the earth's surface. *Arch. Meteorol. Geophys. Bioklimatol. Ser. B* **1956**, *7*, 165–189. [CrossRef]

35. Galván, L.; Olías, M.; Fernandez de Villarán, R.; Domingo Santos, J.M.; Nieto, J.M.; Sarmiento, A.M.; Cánovas, C.R. Application of the SWAT model to an AMD-affected river (Meca River, SW Spain). Estimation of transported pollutant load. *J. Hydrol.* **2009**, *377*, 445–454. [CrossRef]

36. Galván, L.; Olías, M.; Izquierdo, T.; Cerón, J.C.; Fernández de Villarán, R. Rainfall estimation in SWAT: An alternative method to simulate orographic precipitation. *J. Hydrol.* **2014**, *509*, 257–265. [CrossRef]

37. Caissie, D.; El-Jabi, N.; Satish, M.G. Modelling of maximum daily water temperatures in a small stream using air temperatures. *J. Hydrol.* **2001**, *251*, 14–28. [CrossRef]

38. Willmott, C.J.; Matsuura, K. Advantages of the mean absolute error (MAE) over the root mean square error (RMSE) in assessing average model performance. *Clim. Res.* **2005**, *30*, 79–82. [CrossRef]

39. Cánovas, C.R.; Olías, M.; Nieto, J.M.; Galván, L. Wash-out processes of evaporitic sulfate salts in the Tintoriver: Hydrogeochemical evolution and environmental impact. *Appl. Geochem.* **2010**, *25*, 288–301. [CrossRef]

40. Stumm, W.; Morgan, J.J. *Aquatic Chemistry, Chemical Equilibra and Rates in Natural Waters*, 3rd ed.; Wiley: New York, NY, USA, 1996; p. 1022. ISBN 0-471-51184-6.

41. Sarmiento, A.M.; Olías, M.; Nieto, J.M.; Cánovas, C.R. Hydrochemical characteristics and seasonal influence on the pollution by acid mine drainage in the Odiel river Basin (SW Spain). *Appl. Geochem.* **2009**, *24*, 697–714. [CrossRef]

42. Sanchez España, J.; Lopez Pamo, E.; Santofimia, E.; Aduvire, O.; Reyes, J.; Barettino, D. Acid mine drainage in the Iberian Pyrite Belt (Odiel river watershed, Huelva, SW Spain): Geochemistry, mineralogy and environmental implications. *Appl. Geochem.* **2005**, *20*, 1320–1356. [CrossRef]